Mass and Energy Transfer between a Confined Plasma Jet and a Gaseous Coolant

DEAN L. SMITH, ROBERT H. KADLEC, and STUART W. CHURCHILL

University of Michigan, Ann Arbor, Michigan

Mass and energy transfer between confined plasma and coolant gas streams was studied experimentally. Argon was used as the plasma gas and nitrogen was used as the coolant gas. The temperature profiles present in the mixing region were determined by optical-spectrographic methods. Both the electronic excitation temperature of the argon atoms and the rotational temperatures of the nitrogen molecules were determined. The compositions and axial velocities present in the plasma coolant mixing region were determined by sampling probe methods.

The measured nitrogen temperatures were found to be much lower than the argon temperatures present at the same point in the flow. The difference could be explained on the basis of incomplete mixing and thermal equilibration on the microscopic scale. The composition profiles indicated that direct induction of coolant into the high-velocity plasma jet and the formation of a recirculation eddy increased the mixing of plasma and coolant.

From the standpoint of carrying out a chemical reaction in the plasma jet, the results indicate that the mixing of a reactant injected into a plasma jet reaction chamber with the plasma would be very rapid but that the internal energy modes of the reactant molecule might not be fully excited during the short residence time in the high-velocity flow.

Although the use of plasmas, or partially ionized gases, for chemical synthesis is not new, interest has greatly increased during the past few years. The interest appears to have been stimulated by the improved generation and diagnostic techniques developed in connection with missile reentry simulation. Unfortunately, most of these diagnostic techniques have not been applied in the high-temperature reaction zone of plasma jet chemical reactors. Instead overall mass and energy balances have been relied upon to infer what happened in the reaction zone. The present study was undertaken to gain some insight into the mass and energy transfer mechanisms occurring in a plasma jet system. Nonreactive gases were used to simplify the analysis.

SCOPE OF WORK

A typical arrangement used for plasma jet chemical synthesis is to use an inert gas such as argon for the plasma jet and mix the reactants with the plasma in a downstream mixing chamber (*1* to *4*). The experimental geometry was chosen to be representative of such reactor systems.

An axially symmetric plasma jet was introduced into a surrounding concentric, concurrent flow of coolant (analogous to reactant) gas. The resulting flow system was confined in a quartz tube. The plasma generator was of the direct-current arc type and was operated with axial flow through the arc region. Argon was used as the plasma gas and nitrogen was used as the coolant gas. The plasma and coolant mixing took place at atmospheric pressure.

The temperature profiles present in the mixing region were determined by optical-spectrographic methods. The electronic excitation temperature of the argon atoms was determined from the absolute intensities of lines in the emission spectra of the atoms. The rotational temperature of the nitrogen molecules was determined from the distribution of intensities in the electronic vibrational-rotational bands of neutral and singly ionized nitrogen molecules. Temperature was defined on the basis of the Maxwell-Boltzmann distribution of population among energy states. Thus a temperature value could be assigned to any energy system which possessed a Maxwell-Boltzmann distribution of state populations.

The compositions and axial velocities present in the plasma coolant mixing region were determined by sampling probe methods.

EXPERIMENTAL EQUIPMENT

The plasma generator was of the direct-current arc type. The design of the generator, as shown in Figure 1, is typical of many generators in use. The plasma forming gas was passed through an arc struck between the cylindrical tungsten cathode and the an-

Dean L. Smith is with Esso Research and Engineering Company, Linden, New Jersey. Stuart W. Churchill is at the University of Pennsylvania, Philadelphia, Pennsylvania.

nular copper anode. The arc power was supplied by a motor-generator set capable of 40 v. at 600 amp. In contrast to most commercially built plasma generators, the plasma gas was given no tangential velocity components before passing through the arc region. The axial flow produced a steady, symmetrical plasma.

The anode was held in place by the plasma coolant mixing chamber, which is shown in Figure 2. It was necessary to line the plasma jet nozzle with copper in order to obtain adequate cooling. The inside diameter of the resulting nozzle was 11 mm.

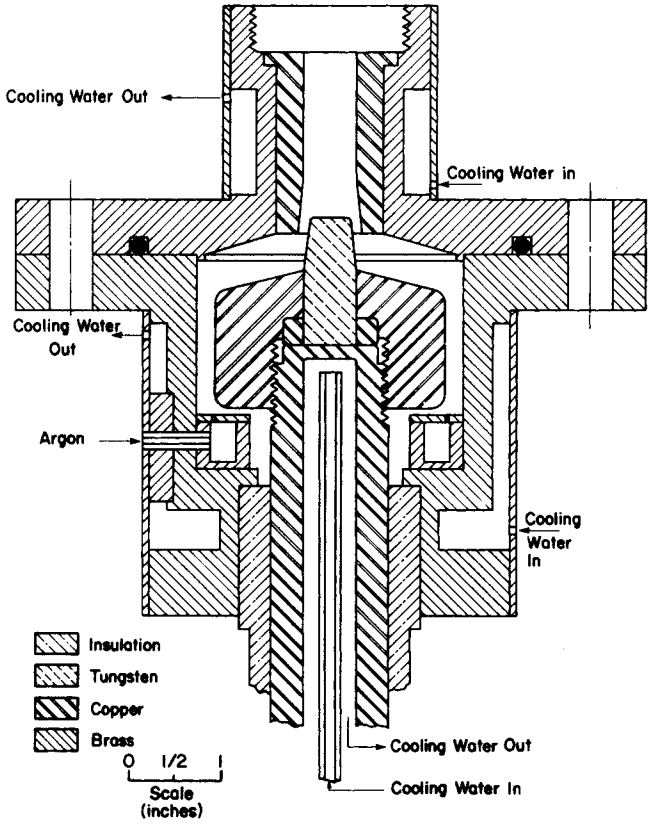

Fig. 1. Arc plasma generator.

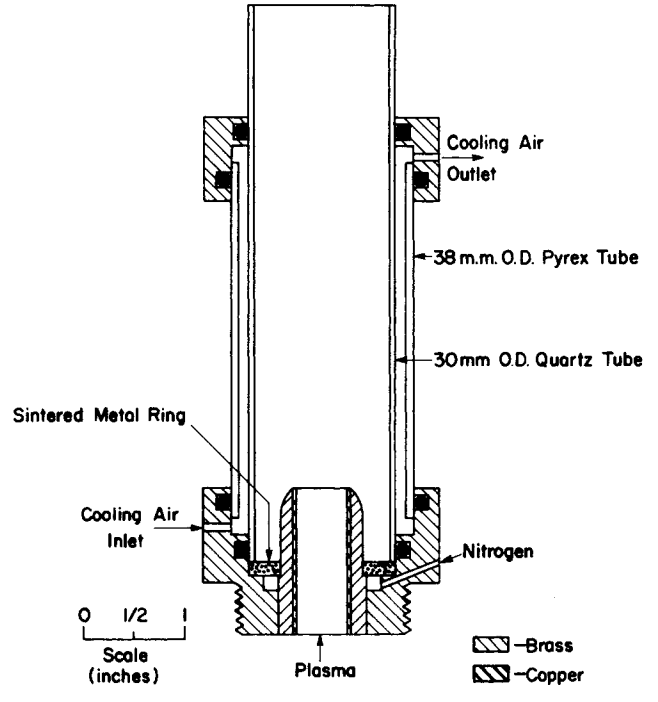

Fig. 2. Plasma coolant gas mixing chamber.

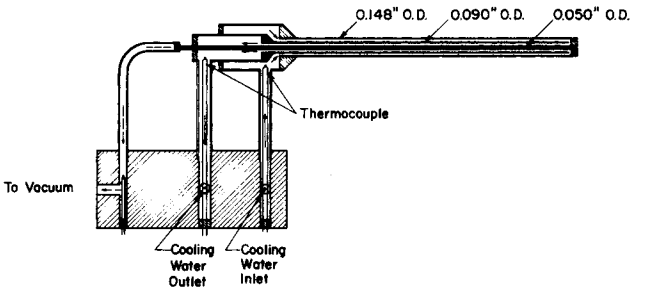

Fig. 3. Water-cooled sampling probe.

The nitrogen gas entered the mixing chamber through an annular porous stainless steel ring around the plasma nozzle. The plasma jet and nitrogen flow were confined inside the 27-mm. I.D. quartz tube. The tube was approximately 5 in. long. This length was selected to prevent organ-pipe resonance with the 2,000 cycle ripple component present in the power supply and plasma. The quartz mixing chamber was cooled by forcing air through the annular space between the mixing chamber tube and the outer Pyrex tube. During operation, the upper portion of the quartz tube was just incandescent. The plasma generator and mixing chamber were capable of indefinitely long operation.

The emission spectra of the argon atoms and nitrogen molecules were analyzed with a 3.4-m.-focal-length-plane grating spectrograph manufactured by the Jarrell-Ash Company. The spectra was recorded on Eastman Kodak type 103a-F spectrographic plates. Line intensities were then determined from the densities of the silver deposits on the plates (*5*).

The sampling probe used consisted essentially of a pitot tube equipped with a cooling water jacket. The probe is shown in Figure 3. For making velocity measurements, the probe functioned like a conventional pitot tube. An inclined water manometer was used to measure the impact pressures. For making composition measurements, a sample of gas was continuously withdrawn from a desired location in the plasma flow. The sample was then passed through a thermal conductivity cell for analysis. The probe, which was 3.5 mm. in diameter, could remain anywhere within the plasma indefinitely. Chludzinski (*6*) and Grey (*7*) have used similar probes in plasmas. Grey also used his probe to make enthalpy measurements but in the present work such measurements were found to be unreliable.

MEASUREMENT THEORY

In the visible and ultraviolet region, the spectra of atoms and molecules are produced by transitions between the electronic energy levels of the atoms or molecules. For an atom, the intensity I of a spectral line is given by (*8*)

$$I = \frac{1}{4\pi} L h N_0 \nu_{nm} A_{nm} \frac{g_n}{g_0} \frac{1}{Q_e} \exp(-E_n/kT) \qquad (1)$$

where ν_{nm} is the frequency of the photon produced by transition from level n, having energy E_n, to level m. The Einstein probability of spontaneous transition A_{nm} is different for each pair of energy levels. In theory this transition probability is calculable from quantum mechanics, but in practice it must be determined experimentally. Adcock (*9*) has tabulated the determinations of a number of investigators for the principal spectral lines of argon. For argon the statistical weight g_0 of the ground electronic level is unity and for the temperatures encountered in this work (below 10,000°K.) the electronic partition function Q_e is also unity. Since argon is less than 1% ionized below 10,000°K. (*10*), the number density of argon atoms N_0 can be calculated from the ideal gas law. Except for the temperature T, the other quantities in Equation (1) are known constants. Thus from the measured absolute intensity of a spectral line, the temperature can be calculated. This temperature is the electronic excitation temperature of the argon atoms. In atmospheric pressure argon plasmas, calculations (*11*) and experiments (*12*) indicate that the atomic excitation

temperature is also representative of the other energy modes, that is, translation and ionization. Because of the exponential dependence of intensity upon temperature, large errors in the measurement of intensity produce only small percentage errors in the calculated temperatures. In the present work a total uncertainty of 34% in the transition probabilities and measured intensities resulted in a 2% uncertainty in temperature.

In molecules, each electronic energy level is increased by small increments because of interaction with the vibrational and rotational energy modes of the molecule. Thus the spectra of molecules consist of bands of lines. A given band consists of lines produced by transitions between the same electronic and vibrational levels. The distribution of line intensities within a band is related to the rotational temperature of the molecule. The intensity of a given line in emission is given by Herzberg (*13*):

$$I = \frac{C\nu^4}{Q_r} S_J \exp\left[-B_v J(J+1)hc/kT\right] \qquad (2)$$

where C is a constant dependent upon the total number of molecules in the initial vibrational level and upon the quantum mechanical transition moment. Q_r is the rotational partition function and is a constant. B_v is a function of the initial electronic and vibrational states; it is inversely proportional to the moment of inertia of the molecule. An extensive tabulation of B's is given in reference *13*. The rotational quantum number J is known as soon as a given line in the band is identified. The lines of the nitrogen bands used in this work have been tabulated by Coster (*14*) and Fassbender (*15*). The line strength S_J is a function of J which depends upon the type of transition taking place. The appropriate nitrogen line strengths are given by Herzberg and by Budo (*16*). Since the absolute value of the constant C was not known, the distribution of line intensities within the band had to be used to determine the temperature. This was done graphically by plotting the relative intensities of the lines versus their corresponding rotational quantum numbers. The rotational temperature of the molecules was then determined from the shape or slope of the resulting curve. The details of the application of this method to both neutral and singly ionized nitrogen molecules are given in reference *5*. The rotational temperature determinations had an estimated accuracy of ±20%.

The spectrograph recorded all of the radiation coming along a chord passed through the plasma source. The lateral intensity which it recorded is equivalent to the integral of the various intensities along the chord. In an axial symmetric source which contains temperature gradients, the intensity actually has a radial distribution. It was thus necessary to convert the observed lateral intensities into true radial intensities. The method of Nestor and Olsen (*17*) was used for this conversion.

The sampling probe measurement of plasma compositions is straightforward, but the measurement of velocity requires some discussion. The free stream velocity is calculated by application of the Bernoulli energy equation

$$V_2^2 - V_1^2 = -2\int_1^2 \frac{1}{\rho}\, dp \qquad (3)$$

In the equation, ρ is the fluid density, p the hydrodynamic pressure, and V the velocity. When applied to a pitot tube, V_1 is the free stream velocity, V_2 is zero, and p varies from the free stream pressure (*1*) to the probe-tip stagnation pressure (*2*). The integral is path dependent. For an isothermal, constant density change its value is $(p_2 - p_1)/\rho$. However, for a water-cooled probe placed in a high-temperature plasma jet, the pressure increase does not occur under constant density conditions.

Under these circumstances the velocity can be calculated from the following equation:

$$p_0 - p_\infty = \frac{\rho_\infty V_\infty^2}{2} + \frac{\rho_\infty^2 V_\infty^4}{8\kappa_\infty p_\infty} + \frac{2\mu V_\infty}{R\left(1 + \dfrac{0.455}{\sqrt{N_{Re}}}\right)} \qquad (4)$$

The details of the derivation of this expression are given in reference *18*. The first two terms are the Bernoulli term and the compressibility term, respectively, and are evaluated at the free stream temperature. The third term is the viscous effect, and is evaluated at a reference temperature defined to be the temperature corresponding to mean enthalpy.

RESULTS

A number of different plasma and coolant flow rates were used during the work. The ones discussed in detail here are listed in Table 1. Operation with the argon flow rate of 58.7 g./min. produced a stable, symmetrical, reproducible plasma. The jet Reynolds number, based upon average viscosity, was approximately 800 but the plasma jet was considered to be in turbulent flow due to the extreme turbulence in the arc itself, immediately upstream. The argon profiles for flow condition 1 are shown in Figure 4. The coordinate system used measured radial position r from the center line of the jet and axial position z from the downstream edge of the plasma nozzle. The jet was not luminous beyond an axial distance of 3.0 cm. In Figure 4 the argon temperature measurements beyond 5 mm. are no doubt due to scattering, backmixing of gas, and possibly reflections from the quartz wall. The temperature profiles for flow conditions 2 and 3 were similar. The nitrogen temperature profiles for flow condition 1 are shown in Figure 5. Again, the temperature profiles were similar for the other flow conditions. The temperatures determined from the N_2 and N_2^+ molecules agree reasonably well. The uncertainties were estimated to be ±2%.

Comparison of Figure 4 with Figure 5 reveals that the determined argon and nitrogen rotational temperatures are different at the same point within the plasma. Before advancing reasons for the difference, the validity of the determinations needs to be established. The mass and energy balances which are discussed below were one source of verification. Spectrographic results were another source of verification. When the nitrogen was passed through the electric arc along with the argon, atomic nitrogen lines were visible in the spectra indicating a high temperature. When the nitrogen mixed only with the argon plasma, no atomic nitrogen lines were visible even though the overall nitrogen concentration at the points observed was greater.

To gain insight into the energy transfer mechanism between the argon atoms and nitrogen molecules, their collision frequency was calculated on the basis of the hard sphere approximation. Benson (*19*) gives equations for calculating the collision frequency between molecules having Maxwellian velocity distributions. The calculations indicated that a nitrogen molecule would undergo approximately 8×10^4 collisions between the time it entered the plasma jet and the time that it was observed at an axial distance of 2.0 cm. On the basis of the hard sphere model,

TABLE 1. FLOW CONDITIONS STUDIED (PRESSURE = 1 ATM.)

Designation	Flow rates: Argon plasma (g./min.)	Flow rates: Nitrogen coolant (g./min.)	Net energy content (kw.)
1	58.7	1.90	3.06
2	58.7	8.22	3.06
3	58.7	18.4	3.15

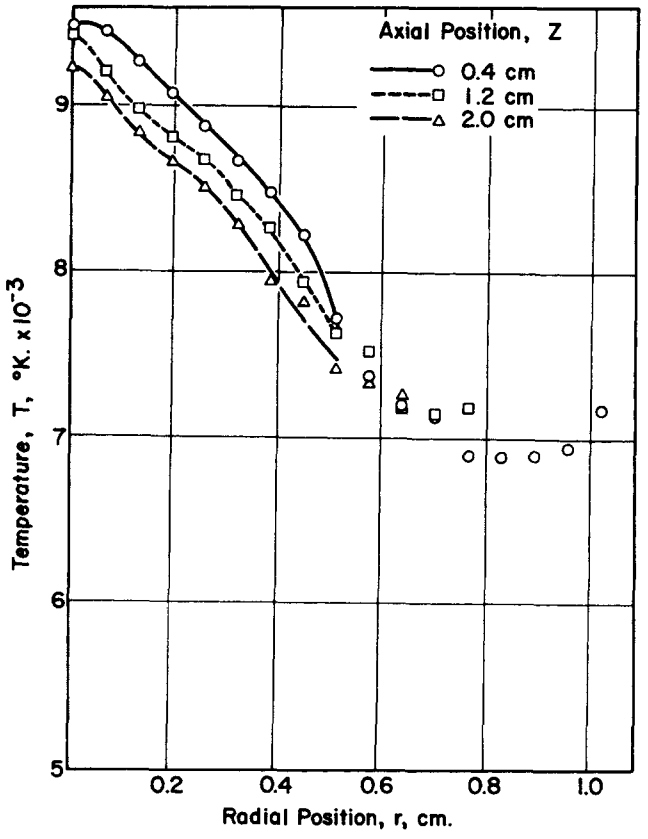

Fig. 4. Argon temperature versus position for flow condition 1.

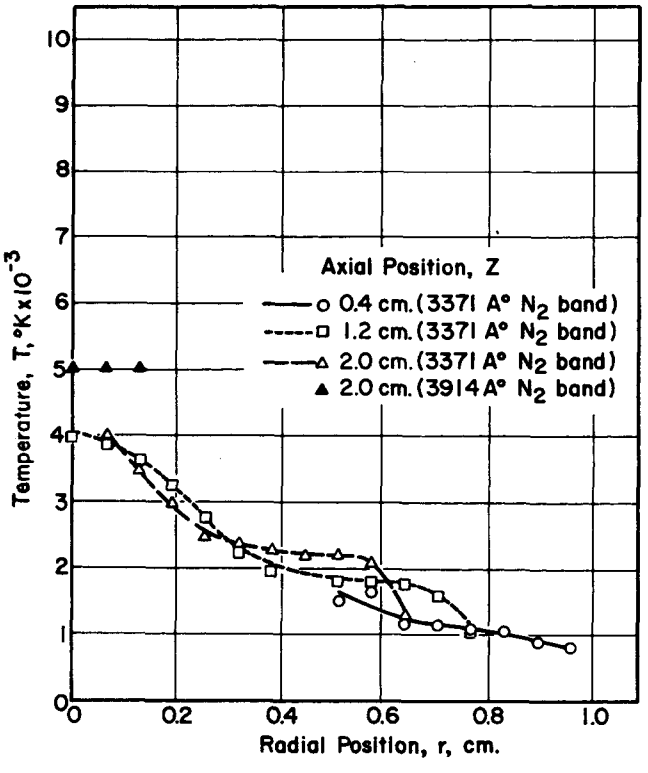

Fig. 5. Nitrogen temperature versus position for flow condition 1.

the nitrogen would have been able to exchange enough energy with the argon for equilibrium to have been reached.

A possible explanation for these low nitrogen temperatures lies in the nature of the mixing which takes place in the jet. If a large amount of nitrogen is entrained and recirculates, it is almost certain that turbulence exists. In such a situation, mixing is likely to occur via the motion of microscopic "packets" of gas. The contents of such a packet would constitute an isolated system which would equilibrate by the process of thermal diffusion. The number of highly energetic argon atoms which penetrated these packets to produce thermal equilibration via mass transfer apparently was insufficient.

The existence of such microscopic entities could not be determined either with the large sampling probe or with spectrographic analysis. In the case of the probe, the mixing in the sample line would tend to destroy the nonuniformity. Any optical measurement would, of necessity, view an average of all the nitrogen molecules in a line-of-sight.

A summary of such micromixing effects is presented by Himmelblau and Bischoff (*20*). In this process, a second-order effect is present, in that collisions between two molecules are required to transmit energy. Calculations presented in reference *20* show that, depending upon whether the flow is perfectly micromixed or completely microsegregated, a factor-of-two difference in the overall result of such a collisional process is possible. In the present case, not enough is known about the type of mixing to rule out this possibility.

The results of the sampling probe composition measurements are shown in Figures 6 through 8. The most interesting feature of the plots is the peak in nitrogen concentration which occurred for flow condition 1. Peaks were also obtained at other plasma flow rates when the nitrogen to argon ratio was low. With cold flow such peaks did not occur for any composition ratio nor have any such peaks been reported in the literature. These peaks will be explained below in connection with induction and recirculation. The composition data are considered accurate to within ±2% and they were reproducible.

The pitot tube determined axial velocity profiles for flow condition 1 are shown in Figure 9. The velocities for the other flow conditions were similar. All of the plasma flow velocities were calculated while using the correction of Equation (4). Both composition and temperature data were used to calculate the required free stream densities. The determinations of the velocities in the high-velocity jet region are considered quite accurate. Outside of this high-velocity region reliable velocities could not be determined

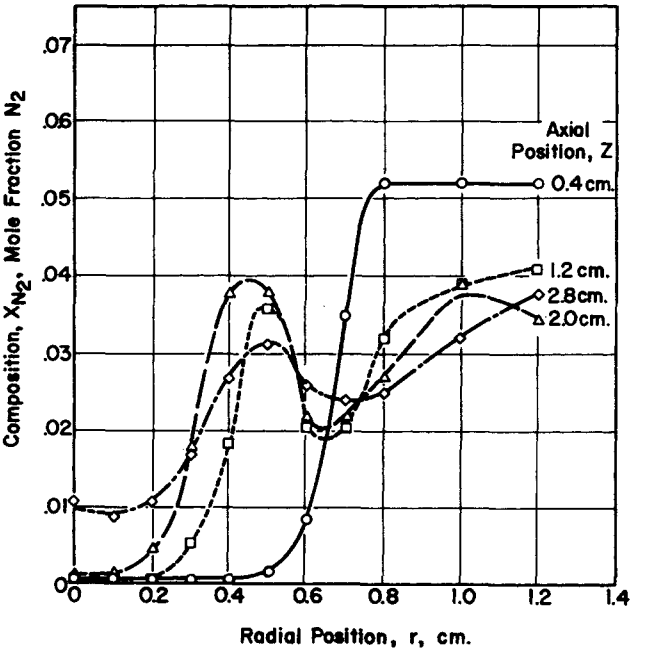

Fig. 6. Composition versus position for flow condition 1.

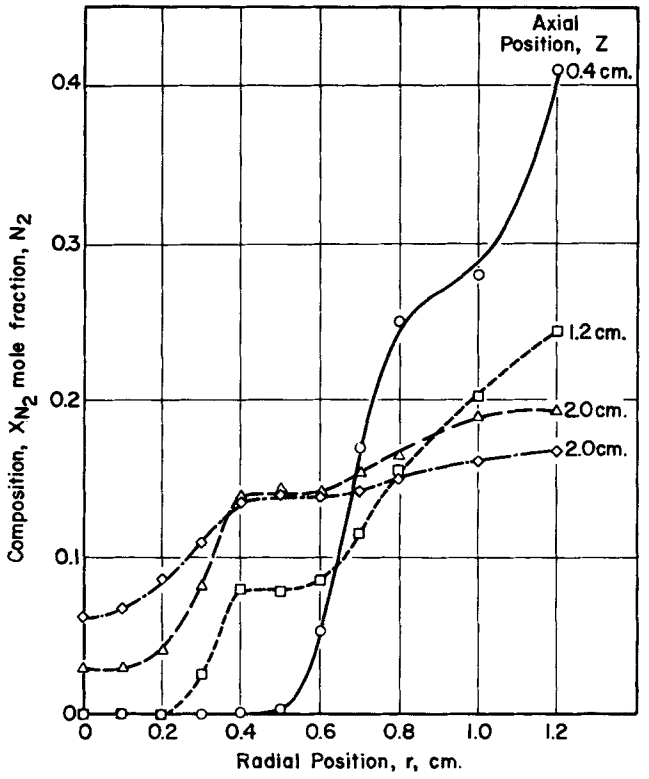

Fig. 7. Composition versus position for flow condition 2.

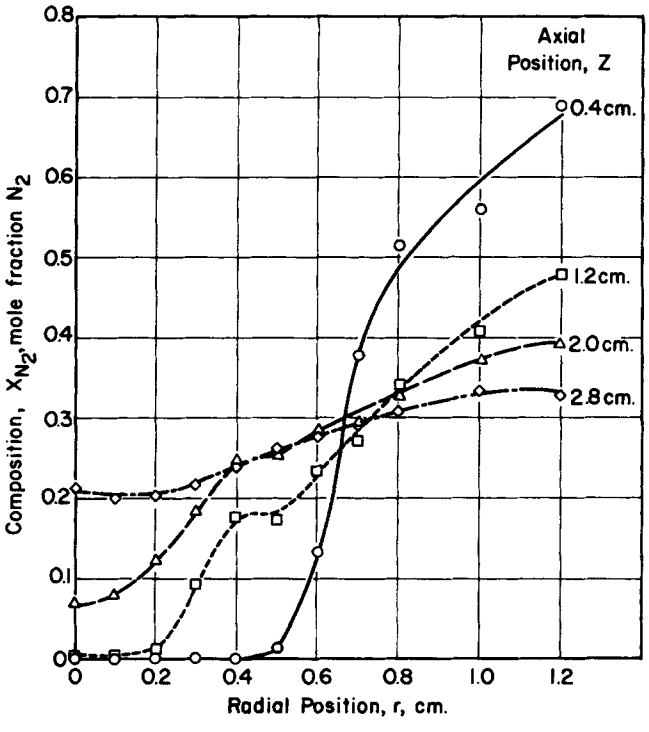

Fig. 8. Composition versus position for flow condition 3.

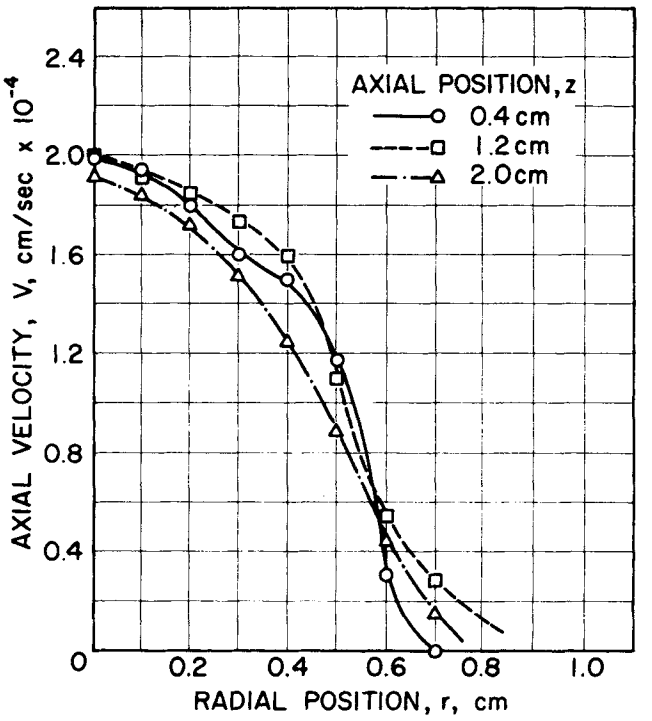

Fig. 9. Axial velocity versus position for flow condition 1.

because of lack of sensitivity in the water manometer used. The sampling probe measured only the stagnation (impact) pressure. For the free stream pressure, which also is required for use in velocity Equation (4), the probe reading at the wall was used. The flow velocity was so low at this point that the impact reading was equivalent to the free stream pressure. As is normal in confined jet work (*21*), the same free stream pressure was used for all radial measurements at a given axial position. For both plasma and cold flow conditions, the free stream pressure was negative (below atmospheric) at all of the axial positions used.

By using the spectrographically determined temperatures and the probe-determined compositions and velocities, mass and energy balances could be made for the plasma flows. A digital computer was used to perform the calculations. Drellishak's data for density and enthalpy were fitted numerically, and the required integrations across the plasma flow were performed by using Simpson's rule. The results of the overall mass and energy balances agreed with the input rates only when the argon temperatures were used for the argon fraction of the flow and the nitrogen temperatures for the nitrogen fraction.

Balances for the nitrogen fraction only indicated that from one-half to three-fourths of the nitrogen coolant was present in the high-temperature region of the flow but that this coolant fraction contained less than 10% of the total energy present.

The observed temperature and composition profiles can be explained on the basis of jet induction (or entrainment) and recirculation. For all plasma flow conditions a large amount of nitrogen coolant appears to be inducted into the argon plasma jet near the start of the mixing region. The nitrogen composition peak caused by this induction is visible in the composition profiles for flow condition 1. The nitrogen to argon composition ratio was very low for this flow condition. For the other flow conditions, greater diffusion caused by the higher concentrations of nitrogen smoothed out the peaks. The gradual change with increasing nitrogen is evident in going between flow conditions 1, 2, and 3. The formation of the peaks shown also requires that argon-rich gas recirculate back to near the start of the mixing region. Additional insight into the flow pattern can be gained from plots of constant composition. Such a plot for flow condition 1 is shown in Figure 10. In regions where flow is controlling the distribution of the gases, the flow lines and lines of constant composition should be parallel. On the basis of the composition-contour plot for flow condition 1, a possible recirculation pattern for this flow condition is shown in Figure 11. Since the manometer used for the pitot tube velocity measurements

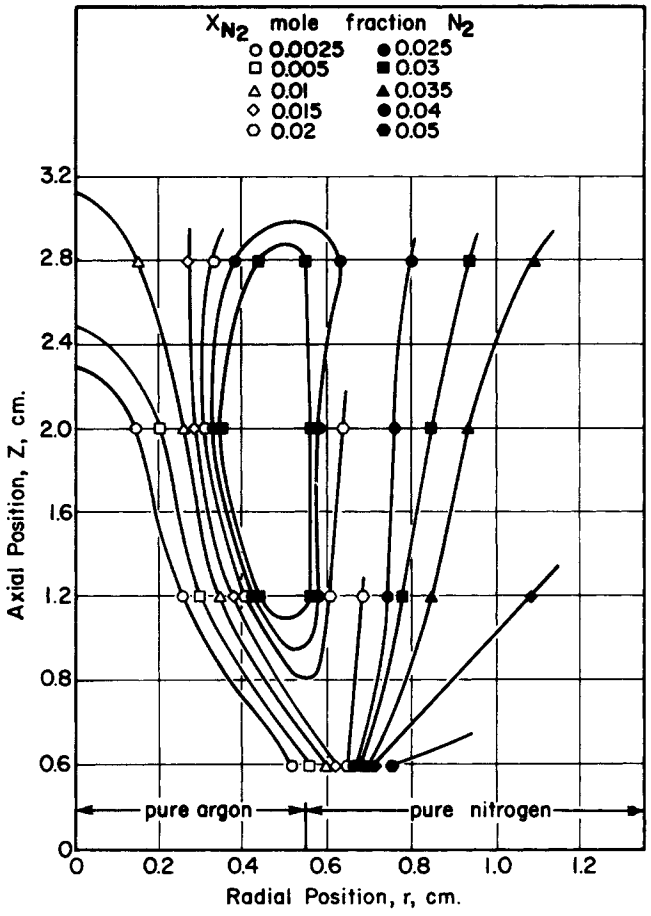

Fig. 10. Contours of constant composition for flow condition 1.

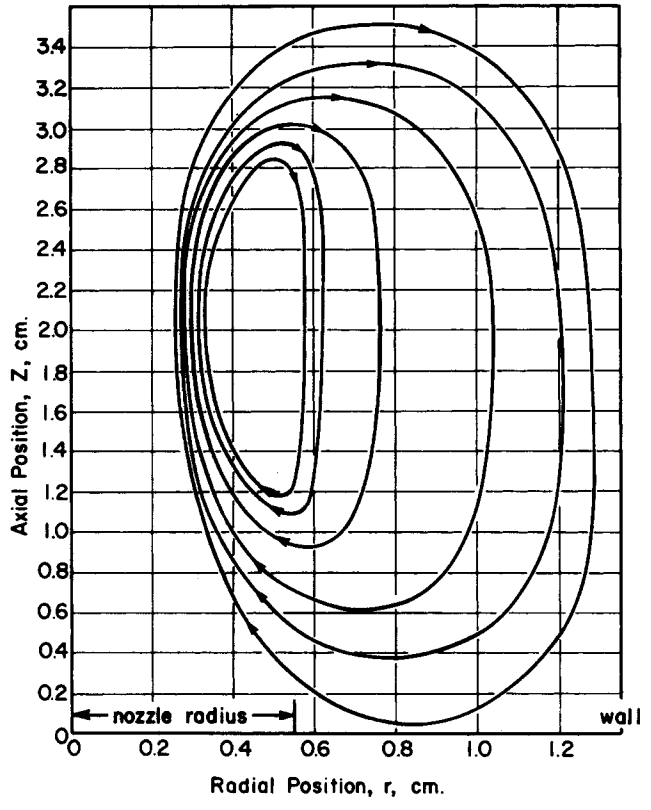

Fig. 11. Possible recirculation pattern for flow condition 1.

was low in sensitivity, the recirculation pattern could not be confirmed by velocity measurements. The dips in the argon temperature profiles at the axial distances of 1.2 and 2.0 cm. can be explained on the basis of induction of large amounts of cool nitrogen into the jet near its axis. The temperature profiles are thus affected by the flow pattern in addition to the usual diffusion and conduction mechanisms.

Some confined jet research which has been conducted at ordinary temperatures can be used to support the induction and recirculation conclusions. Ricou and Spalding (22) experimentally studied entrainment in axially symmetric gas jets of various densities. At axial distances z much larger than the diameter of the jet nozzle R_1, they found the mass of fluid entrained to be

$$w_1 \left[0.32 \frac{z}{R_1} \left(\frac{\rho_2}{\rho_1}\right)^{1/2} - 1\right] \tag{5}$$

where w_1 is the mass flow rate of the jet. The subscripts 1 and 2 refer to the jet and surrounding fluid, respectively. From Equation (5) the amount of nitrogen entrained by the plasma jet up to an axial distance of 2.0 cm. would be 22.3 g./min. Thus for all flow conditions the jet was capable of entraining more than the entire nitrogen coolant flow. A recirculation eddy would then supply the remainder of the entrainment capacity.

Becker (23) has made a general analysis of recirculation in confined jets. He has developed a parameter N_{Ct} called the Craya-Curtet number, whose value is a criterion for the occurrence of recirculation. For a cylindrical constant density system the parameter is defined as

$$N_{Ct} = \left[\frac{R_1^2(V_1^2 - V_2^2) + \dfrac{V_2^2 R_2^2}{2}}{Q_t^2/\pi^2 R_2^2} - \frac{1}{2}\right]^{-1/2} \tag{6}$$

Since the Craya-Curtet number was derived for constant density systems, Equation (6) had to be modified to include the effects of different source and secondary flow densities. Since the momentum of the streams is actually of interest, all of the velocity terms were multiplied by their related densities. Average jet and secondary velocities were used. For flow conditions 1, 2, and 3, the Craya-Curtet numbers were found to range from 0.44 to 0.52. Becker experimentally found that recirculation occurred for N_{Ct} less than 0.75. Thus recirculation would be expected for all three flow conditions.

From a chemical reaction standpoint, the induction and recirculation phenomena make it unimportant how the reactants are injected into the mixing chamber. Either radial or axial introduction should have about the same effect. Such an observation is consistent with the experimental findings of Biggerstaff (2).

A simplified version of the differential equation which describes the mixing of the plasma and coolant by flow and diffusion was solved. Constant radial and axial velocities and diffusion coefficient were assumed. Axial concentration gradients were neglected. When radial and axial velocities equivalent to the recirculation pattern shown in Figure 11 were used, peaks were obtained in the composition profiles for flow condition 1. The solution was very dependent upon the exact radial velocities used. Because of lack of knowledge about the true recirculation and induction velocities, no effort was made to duplicate the experimentally determined composition profiles. For flow condition 3, which had a high nitrogen to argon ratio, good duplication of the experimentally determined composition profiles could be obtained by using only axial velocities (no recirculation) and an effective diffusion coefficient of 200 sq. cm./sec.

Levenspiel (*24*) presents correlations for effective diffusion (dispersion) coefficients. The correlations actually are for uniform flow through a pipe, but if plasma and coolant velocities were averaged across the mixing tube, order of magnitude agreements with the correlations were obtained for both flow condition 3 and cold flow conditions. The viscosity used was that of the jet. Laminar diffusion coefficients and thermal diffusion ratios for argon and nitrogen at high temperatures are given by Amdur (*25*). The coefficients listed are much smaller than the 200 sq. cm./sec. found above. Thus turbulent diffusion is predominant.

SUMMARY AND CONCLUSIONS

Mass and energy transfer between confined argon plasma jet and nitrogen coolant streams was studied experimentally. The measured nitrogen temperatures were found to be much lower than the argon temperatures present at the same point in the flow. The difference could be explained on the basis of the incompleteness of the micromixing process. Composition profiles indicated that direct induction of coolant into the high-velocity plasma jet and the formation of a recirculation eddy greatly increased the mixing of plasma and coolant. The induction and recirculation phenomena were found to be consistent with correlations developed for confined jets at ordinary temperatures. Mass and energy balances computed at various axial distances in the mixing region indicated that from one-half to three-fourths of the nitrogen coolant was present in the high-temperature region of the flow but that this coolant fraction contained less than 10% of the total energy present. Total mass and energy balances based upon the different argon and nitrogen temperatures agreed with the input rates and thus confirmed the accuracy of the temperature measurements. The solution of the differential equation describing argon-nitrogen diffusion indicated that flow and turbulent diffusion controlled the mixing of the plasma and coolant.

The results of this study indicate that gross mixing of a reactant injected into a plasma jet reaction chamber with the plasma would be very rapid but that the internal energy modes of the reactant molecule would not be fully excited during the short residence time in the high-velocity flow.

ACKNOWLEDGMENT

The financial support of this work by National Science Foundation Grant GP 331 was greatly appreciated.

NOTATION

A_{nm} = Einstein transition probability for spontaneous transition from level n to level m, sec.$^{-1}$
B_v = rotational constant for vibrational level v
c = velocity of light, cm./sec.
C = constant in Equation (2)
E = energy, ergs
g = statistical weight
h = Planck's constant, ergs/sec.
I = absolute intensity of radiation, ergs/(sec.)(sq. cm.)(sterad)
J = rotational quantum number
k = Boltzmann constant, ergs/°K.
L = source thickness, cm.
N = number density, 1/cu. cm.
N_{Ct} = Craya-Curtet number as defined in Equation (6)
N_{Re} = Reynolds number, based on R and V_∞
p = pressure, dynes/sq. cm.
Q = partition function
Q_t = total volumetric flow rate, cu. cm./sec.
r = radial coordinate, cm.
R = probe radius, cm.
R_1 = jet source radius, cm.
R_2 = radius of mixing tube, cm.
S_J = line strength
T = temperature, °K.
v = vibrational quantum number
V = axial velocity, cm./sec.
V_1 = jet source average velocity, cm./sec.
V_2 = secondary flow average velocity at $z = 0$, cm./sec.
w = flow rate, g./min.
z = axial coordinate measured from source, cm.

Greek Letters

μ = viscosity, poise
ν = frequency, 1/sec.
ρ = fluid density, g./cu. cm.
κ = heat capacity ratio

Subscripts

e = electronic
m = lower energy level
n = upper energy level
r = rotational
v = vibrational
0 = ground state, stagnation point
1 = primary flow (jet source)
2 = secondary flow (coolant)
∞ = free stream conditions

LITERATURE CITED

1. Freeman, M. P., and J. F. Skrivan, *AIChE J.*, **8**, 450 (1962).
2. Biggerstaff, G. E., W. R. Golliher, R. L. Harris, and W. R. Rossmassler, *AEC Res. Develop. Rept. KY-453* (Feb. 1964).
3. Anderson, J. E., and L. K. Case, *Ind. Eng. Chem. Process Design Develop.*, **1**, 161–165 (July 1962).
4. Marynowski, C. W., R. C. Phillips, J. R. Phillips, and N. I. Hiester, *Ind. Eng. Chem. Fundamentals*, **1**, 52–61 (Feb. 1962).
5. Smith, D. L., Ph.D. thesis, Univ. Michigan, Ann Arbor (1965).
6. Chludzinski, G. R., Ph.D. thesis, Univ. Michigan, Ann Arbor (1964).
7. Grey, J., and P. F. Jacobs, *AIAA J.*, **2**, 433–438 (1964).
8. Pearce, W. J., in "Optical Spectrometric Measurements of High Temperatures," P. J. Dickerman, ed., pp. 125–169, Univ. Chicago Press, Chicago (1961).
9. Adcock, B. D., and W. E. Plumtree, *J. Quant. Spectrosc. Radiat. Transfer*, **4**, 29–39 (1964).
10. Drellishak, K. S., C. F. Knoop, and A. B. Cambel, *Phys. Fluids*, **6**, 1280–1288 (1963).
11. Williams, P. M., M. P. Sherman, and P. F. Jacobs, *Princeton Univ. Aeronaut. Eng. Rept. No. 651* (June 1963).
12. Olsen, H. N., in "Temperature: Its Measurement and Control in Science and Industry," C. M. Herxfeld, editor-in-chief, Vol. 3, pp. 587–592, Reinhold, New York (1962).
13. Herzberg, G., "Molecular Spectra and Molecular Structure. I. Spectra of Diatomic Molecules," D. Van Nostrand, Princeton, N. J. (1950).
14. Coster, D., F. Brons, and A. Van der Ziel, *Z. Phys.*, **84**, 304–334 (1933).
15. Fassbender, M., *ibid.*, **30**, 73–92 (1924).
16. Budo, A., *ibid.*, **105**, 579–587 (1937).
17. Nester, O. H., and H. N. Olsen, *Soc. Ind. Appl. Math.*, **2**, 200–207 (1960).
18. Carleton, F. E., Ph.D. thesis, Univ. Michigan, Ann Arbor, 1970.
19. Benson, S. W., "The Foundations of Chemical Kinetics," pp. 135–167, McGraw-Hill, New York (1960).
20. Himmelblau, D. M., and K. B. Bischoff, "Process Analysis and Simulation," Wiley, New York (1968).
21. Abramovich, G., "The Theory of Turbulent Jets," p. 635, Massachusetts Inst. Technol. Press, Cambridge (1963).
22. Ricou, F. P., and D. B. Spalding, *J. Fluid Mech.*, **11**, 21–32 (1961).
23. Becker, H. A., H. C. Hottel, and G. C. Williams, "Ninth Symposium on Combustion—1962," p. 7, Academic Press, New York (1963).
24. Levenspiel, O., "Chemical Reaction Engineering," p. 276, Wiley, New York (1962).
25. Amdur, I., *AIChE J.*, **8**, 521–526 (1962).

Manuscript received September 18, 1968; revision received August 18, 1969; paper accepted August 22, 1969.